Machine Copy for Proofreading, Vol. x, y–z, 2011

MULTI-SCALE APPROACH FOR THE ELECTROMAGNETIC SIMULATION OF FINITE SIZE AND THICK FREQUENCY SELECTIVE SURFACES

E. B. Tchikaya, F. Khalil, F. A. Tahir, and H. Aubert †

CNRS, LAAS
7 Avenue Du Colonel Roche, Toulouse Cedex 4 F-31077, France

Abstract—The scattering analysis from metallic Grid FSS consisting of rectangular perforations on a thick metallic screen illuminated by an oblique incident plane wave is presented. The grid structure is analyzed using Scale Changing Technique (SCT) which is based on the partition of the grid-plane into planar sub-domains defined at various scale-levels. Electromagnetic interaction between subsequent scales is modeled by mutually independent Scale-Changing Networks and finally the complete structure is simply represented by a cascade of these networks. Very good agreement is obtained between simulation results from SCT and the Finite Element Method (FEM) when computing the reflection/transmission coefficients and electromagnetic field backscattered by thick and finite size frequency selective surfaces. The computation time is significantly reduced when using SCT-based software compared with the FEM simulation tool.

1. INTRODUCTION

The accurate prediction of the electromagnetic scattering by finite size arrays is of great practical interest in the design and optimization of modern frequency selective surfaces (FSSs), reflect-arrays and transmit-arrays. A complete full-wave analysis of these structures requires generally enormous computational resources due to their large electrical dimensions which would require prohibitively large number of unknowns to be solved. The unavailability of efficient and accurate design tools for these applications limits the engineers with the choice of low performance simplistic designs that do

Received 14 January 2011.
Corresponding author: Farooq Ahmad Tahir (fatahir@laas.fr).
† All are also with UPS, INSA, INP, ISAE; UT1, UTM, LAAS, University of Toulouse, Toulouse Cedex 4 F-31077, France.

not require enormous amount of memory and processing resources. Moreover the characterization of large array structures would normally require a second step for optimization and fine-tuning of several design parameters since the initial design procedure assumes several approximations (e.g., in the case of reflectarrays the design is usually based on a single cell scattering parameters under normal incidence) which is not the case practically. Therefore a full-wave analysis of the initial design of the complete structure is necessary prior to fabrication, to ensure that the performance conforms to the design requirements. A modular analysis technique which is capable of incorporating small changes at individual cell-level without the need to rerun the entire simulation is extremely desirable at this stage.

Historically several approaches have been followed when analyzing large planar structures [1]. In the case of uniform arrays, where we have periodicity in the geometry, an infinite approach is often used. By using Floquet theorem, the analysis is effectively reduced to solving for a single unit-cell; thus significantly reducing the unknowns and hence the simulation times [2, 3]. Although the periodic boundary conditions take into account the effect of mutual coupling in the periodic environment, the approximation may not hold for the arrays where individual cell geometries are very different. In addition this is a very poor approximation for the cells lying at the edges of the array. A simple method based on Finite Difference Time Domain (FDTD) technique has been proposed to precisely account for the mutual coupling effects. It consists of illuminating a single cell in the array in the presence of the nearest neighbor cells and calculating the reflected wave. Though it allows precise excitation and boundary conditions for each cell in the array it is not very practical to design large arrays due to extremely long execution times [4]. Different conventional methods have been tested for full-wave analysis of periodic structures, e.g., Method of Moments (MOM) used in the spectral domain for multilayered structures [5, 6], Finite Element Method (FEM) [7] and FDTD [8]. But these methods require prohibitive resources for the cases where the local periodicity assumption cannot be applied. A spectral domain immittance approach has been used in the full-wave analysis of a 2-D planar dipole array along with the Galerkin procedure using entire domain basis functions [9]. The MoM for the global electromagnetic simulation of finite size arrays requires high CPU time and memory especially when the patch geometries are non-canonical and therefore sub-domain basis functions have to be used. The memory problem may be resolved by using various iterative techniques (e.g., Conjugate Gradient iterative approach) [10, 11] at the cost of further increase in the execution time. A promising improvement of the

MoM, called the *Characteristic Basis Method of Moment* was proposed for reducing the execution time and memory storage for large-scale structures [12, 13]. However the convergence of numerical results remains delicate to reach systematically.

In order to overcome the above-mentioned theoretical and practical difficulties, an original monolithic formulation for the electromagnetic modeling of multi-scale planar structures has been proposed [12]. The power of this technique called the *Scale-changing Technique (SCT)* comes from the modular nature of its problem formulation. Instead of modeling the whole planar-surface as a single large discontinuity problem, it is split into a set of many small discontinuity problems, each of which can be solved independently using mode-matching variation methods [13]. Each of the sub-domain discontinuity solution can be expressed in the matrix form characterizing a multiport-network called *Scale-changing Network* (SCN). SCT models the whole structure by interconnecting all SCNs, where each network models the electromagnetic coupling between adjacent scale levels. The cascade of SCN allows the global electromagnetic simulation of all sorts of multi-scaled planar geometries. The global electromagnetic simulation of structures via the cascade of Scale-Changing Networks has been applied with success to the design and electromagnetic simulation of specific planar structures such as multi-frequency selective surfaces of infinite extent [14], discrete self-similar (pre-fractal) scatterers [15, 16], patch antennas [17, 18], planar array structures [19] and reconfigurable phase-shifters [20, 21]. The objective of this work is to apply, for the first time, the SCT in the case of thick and finite size FSS composed of non identical cells.

The present communication is organized as follows: in Section 2 the Scale Changing Technique is applied to the electromagnetic modeling of a thick and finite size FSS. The scattering parameters results and the far-field radiation pattern have been obtained. The conclusions are derived in Section 3.

2. FULL WAVE ANALYSIS OF FSS GRID COMPOSED OF NON IDENTICAL CELLS USING SCALE CHANGING TECHNIQUE

The figure of the proposed FSS is shown in Figure 1(a). It consists of a metallic grid of thickness $h = 5\,\text{mm}$, with 10 mm inter-elements spacing. The dimensions of the apertures are non identical as illustrated. As a first step to demonstrate the potential of the method, we consider the transmission and reflection coefficients of a finite size (256 cells) non-uniform FSS illuminated by a normal incident plane

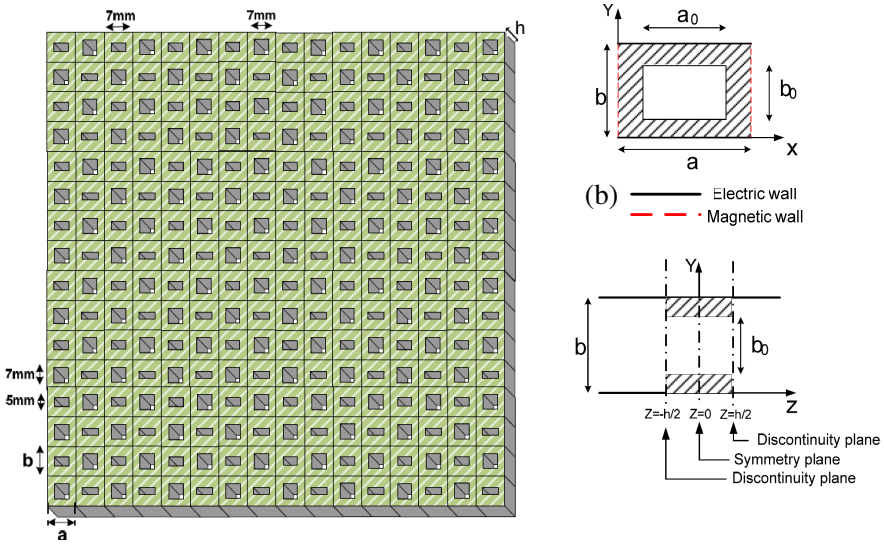

Figure 1. (a) Topology of the FSS consisting of non identical rectangular holes perforating a thick metallic plate; (b) cross section of one cell with its artificial boundary conditions; (c) side-view of the cell. All cells in the grid have the same thickness h.

wave.

Presently the most common method to compute the scattering electromagnetic fields from the planar structures is by solving the integral equation formulation of the Maxwell's equations. This approach permits to express the open boundary electromagnetic problem in terms of an integral equation formulated over the finite planar surface. This reduction of one spatial dimension makes this method very efficient in the case of planar geometries. Yet this method in its traditional formulation is not particularly adapted for large planar structures with scaled geometries and complex metallic patterns. Rapid and fine-scale variations in the structure geometry can cause abrupt changes in electromagnetic field patterns requiring local meshing at a very minute scale which in turn would require immense storage and computational resources. We propose to resolve this problem by introducing local description of the fields for different regions of the planar surface. The procedure can be outlined in the following steps:

1) The planar surface is decomposed in several sub-domain surface regions;
2) The electromagnetic fields are expressed on the modal-basis of

each of these sub-domains bounded by their respective boundary conditions;

3) Modal contributions are treated separately for lower order modes and higher order modes. Higher order modes are considered to contribute only locally where as lower order modes define coupling with the domain at the higher scales;
4) Electromagnetic coupling between two successive scales is modeled by a *scale-changing network* defined by the lower order modes of the two sub-domains;
5) A global electromagnetic solution is obtained by a simple cascade of these scale-changing networks.

These concepts will be explained in further detail in the subsequent sections.

2.1. Theoretical Approach

2.1.1. Partitioning of the Discontinuity Plane

If we consider the discontinuity plane composed of the half-structure (in z-direction), we can easily see that a high scale ratio exists between the highest and the smallest dimensions. The starting point of the proposed approach consists of the coarse partitioning of this (complex) discontinuity plane into large-scale (called scale level $s_{\max}$) sub-domains of arbitrary shape; in each sub-domain a second partitioning is then performed by introducing smaller sub-domains at scale level $s_{\max}-1$; again, in each sub-domain introduced at scale level $s_{\max}-1$ a third partitioning is performed by introducing smaller sub-domains at scale level $s_{\max}-2$; and so on. Such hierarchical domain-decomposition, which allows to focus rapidly on increasing detail in the discontinuity plane, is stopped when the finest partitioning (scale level $s=0$) is reached. An illustration of the partitioning of an FSS with 256 square-waveguide cells (16×16) is sketched in Figure 2; five different scale levels exist when cells are grouped by four, in a regular manner as permitted by the specific structure under investigation to enable some SCN reuse. The partition of this sub-metallic grid in multiple domains Ωs ($s=0,1,2,3,4$) could be performed as follows: the set of 16×16 cells defines the domain Ω_0 and the scale level $s=0$; the domain Ω_0 is composed of 4 domains Ω_1 where Ω_1 defines the scale level $s=1$; Ω_2 defines the scale level $s=2$; the domain Ω_2 is composed of 4 domains Ω_3 where Ω_3 defines the scale level $s=3$ and finally, the domain Ω_3 is composed of 4 domains Ω_4 where Ω_4 defines the scale level $s=4$, that is, the scale of one cell. All these domains have periodic boundary conditions in order to allow the modal representation of co-

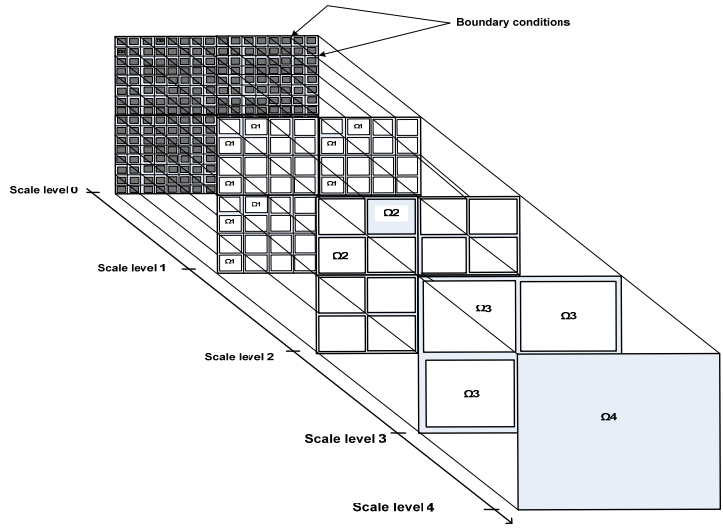

Figure 2. Partitioning into multiple scale levels of the discontinuity plane, i.e., of one side of the thick metallic grid.

and cross-polarized fields at every scale levels (see Figure 2). The next step consists of computing the electromagnetic coupling between two successive scale levels via the SCN. The cascade of SCNs allows crossing the scale from the lowest scale ($s = 0$) to the highest one ($s = s_{\max}$). Thus, we obtain the surface impedance matrix of the entire metallic grid, in the case of even (magnetic wall is inserted in the symmetry plane $z = 0$) and odd (electric wall is inserted in the symmetry plane $z = 0$) symmetries.

2.1.2. Scale Changing Networks [14]

At a given scale level s, the tangential electromagnetic field in the given domain Ω_S combines smooth (large-scale) and highly irregular (fine-scale) variations. The fine-scale variations may be described as the combination of higher-order modes in the domain Ω_S. This combination of higher-order modes is spatially localized and contributes significantly to the representation of the field only in the vicinity of discontinuities and sharp edges.

Consequently these modes do not couple together in the various distant sub-domains included in Ω_S. For this reason, higher order modes are said *passive*. The large-scale contribution to the field is due to distant electromagnetic interaction in the domain Ω_S. This contribution is localized in the modal (spectral) domain. Because they

are involved in the description of the electromagnetic coupling between the various sub-domains of Ω_S, these lower-order modes are called *active* modes.

Moreover, due to their largely different spatial frequencies, any active mode in Ω_S is weakly coupled with any passive mode in the various sub-domains of Ω_S. Consequently it follows from these above-mentioned considerations that the electromagnetic coupling between the domain Ω_S and its constitutive (and distant) sub-domains involves only the active modes.

This coupling may be modeled by the multi-port of Figure 3(a). In this network representation, one port represents one active mode. This multi-port allows to relate the field at scale s (i.e., in Ω_S) to the field at the smaller scale $s-1$ (i.e., in all sub-domains of Ω_S). For this reason, this multi-port is called the *Scale Changing Network*. The determination of the characteristic matrix (i.e., the impedance, admittance or hybrid matrix) of these networks requires the resolution of boundary value problems for which active modes are taken as actual sources. The *Scale Changing Network*s in this case can be viewed as the multiport associated with the bifurcation of Figure 3(b) between a TEM-waveguide (scale $s+1$) and four smaller TEM-waveguides (scale s). The number of active modes at each scale level is chosen by a comprehensive convergence study to precisely define the coupling between two successive scales.

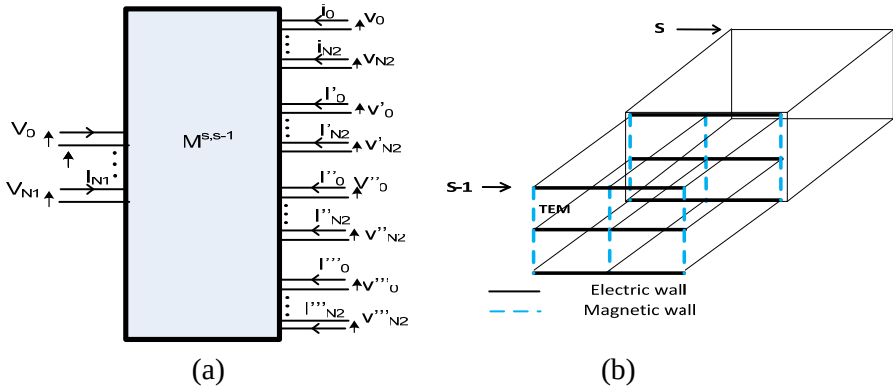

Figure 3. (a) Representation of the electromagnetic coupling between two successive scale levels (i.e., between scale s and $s-1$) by a multiport called the Scale Changing Network. N_1 and N_2 denote respectively the number of active modes at scale $s+1$ and s; (b) the waveguide bifurcation associated with the scale changing.

2.1.3. S-parameters Calculatio

As illustrated in Figure 1(c) the thick metallic grid presents a symmetry plane at $Z = 0$. The grid impedance matrix $[Z_{total}]$ can then be derived from the combination of the two impedance matrices $[Z_{even}]$ and $[Z_{odd}]$ of half-structures obtained by inserting respectively a magnetic wall and electric wall in the symmetry plane, as follows [22]:

$$[Z_{total}] = \frac{1}{2}\begin{bmatrix} [Z_{even}] + [Z_{odd}] & Z_{even}] - [Z_{odd}] \\ [Z_{even}] - [Z_{odd}] & Z_{even}] + [Z_{odd}] \end{bmatrix} \quad (1)$$

The scattering matrix $[S_{total}]$ is then deduced from the following relationship:

$$[S_{total}] = ([Z_{total}] - [Z_0])\,([Z_{total}] + [Z_0])^{-1} \quad (2)$$

where $[Z_0]$ designates the diagonal matrix of active mode impedances. The Scale Changing Technique is applied for the derivation of matrices $[Z_{even}]$ and $[Z_{odd}]$ associated with half-structures.

2.1.4. Unit-cell Multipole

As illustrated in Figure 4(a), surface impedance multiport can be used for modeling the unit-cell (i.e., the smallest scale level). This unit-cell is shown in Figure 4(b) for the magnetic and electric wall configurations. The multimodal multiports $[Z^0_{(mw)}]$ and $[Z^0_{(ew)}]$ modeling the half of unit-cell, respectively when a magnetic wall and an electric wall are inserted in the symmetry plane, are derived by applying the mode-matching technique [22]. The thickness of the metallic grid is thus incorporated at this level of the electromagnetic modeling via these two impedance matrices.

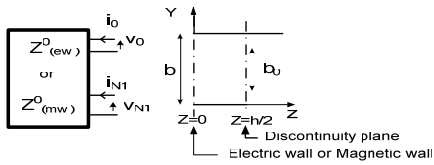

Figure 4. (a) Surface impedance multiport for modeling the unit-cell. N_1 denotes the number of active modes at the smallest scale. (b) Side-view of half of the unit-cell for magnetic and electric wall configurations.

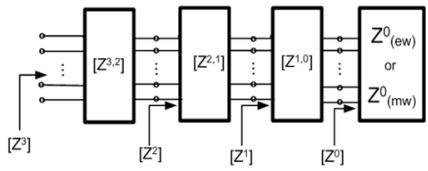

Figure 5. Odd and even multiports at various scale level for modeling FSS consisting of non-identical rectangular apertures perforating a thick and finite sized metallic plate.

2.1.5. Cascade of Scale Changing Networks for Global Electromagnetic Simulation of the Grid

As shown in Figure 5, the cascade of above-derived SCNs allows crossing the scale from the lowest scale ($s = 0$) to the highest one ($s = s_{\max}$). The resulting multi-port is loaded by the smallest-scale surface impedance multiport $[Z^0_{(mw)}]$ for deriving $[Z_{even}]$; it is loaded by $[Z^0_{(ew)}]$ for computing $[Z_{odd}]$. The impedance and scattering matrices of the grid are then deduced from the Equations (1) and (2), respectively.

2.2. Simulation Results

As mentioned before, a number of active modes should be chosen for insuring the numerical convergence of the S-parameters. We have chosen the same number of active modes ($N_1 = N_2 = 70$) at all scale levels. Figure 6 displays the simulated reflection and transmission coefficients of a non-uniform metallic grid (Figure 1(a)) with a thickness $h = 5$ mm in the case of a normal plane wave incidence. Ansoft HFSS (Version 11.1) was used for FEM implementation with 0.02 stopping criterion for the adaptive convergence solution. An excellent agreement between the HFSS- and SCT-results can be observed.

Figure 7 represents the simulation time evolution for these two techniques calculating the transmission and reflection coefficients when the number N of cells increases. For a given grid and simulation technique, the computation time in this figure is normalized to the time required for calculating these coefficients in the case of a 4-cell

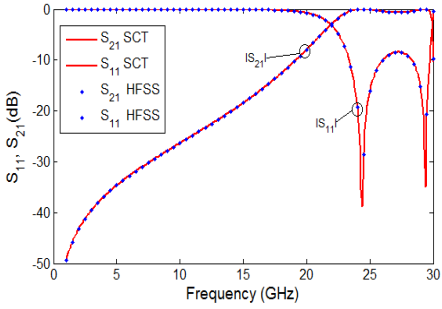

Figure 6. Simulated reflection and transmission coefficients of a 5 mm thick non-uniform 256-cell metallic grid obtained by the SCT and HFSS.

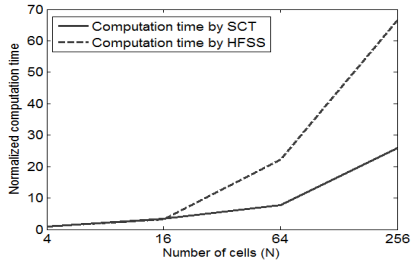

Figure 7. Evolution of computing time compared to the standard time for the calculation of two cells of non uniform arrays.

array. For the Scale Changing Technique computation, time increases very slowly as the number N of cells increases. Meanwhile, in the case of the Finite Element Method, it increases dramatically, because of the mesh refinement needed to insure convergence.

2.3. Radiation Pattern Analysis

We consider the electromagnetic scattering of the plane wave incident on the FSS formed by a thick metallic grid as shown in Figure 8. To calculate the electromagnetic scattering from this planar FSS, one may solve a boundary value problem defined by the following equation:

$$\vec{E}^{total} = Z_s \vec{J}_{eq} \tag{3}$$

that is

$$\vec{E}^{inc} + \hat{G}\vec{J}_{eq} = Z_s \vec{J}_{eq} \tag{4}$$

$\vec{E}^{inc}$ is the incident electric field, and is given by:

$$\vec{E}^{inc} = \begin{cases} E_0 \sin\phi^i e^{-j\left(k_x^i x + k_y^i y\right)\vec{x}} \\ E_0 \cos\phi^i e^{-j\left(k_x^i x + k_y^i y\right)\vec{y}} \end{cases} ; \quad \begin{cases} k_x^i = k \sin\theta^i \cos\phi^i \\ k_y^i = k \sin\theta^i \sin\phi^i \end{cases} \tag{5}$$

where, E_0 is the amplitude and k_x^i, k_y^i are the components of the tangential incident wave vector K. $\vec{J}_{eq}$ is the unknown current density on the metallic domain of the planar scatterer. In the SCT, as shown in Equation (3), we substitute the actual current by an equivalent current

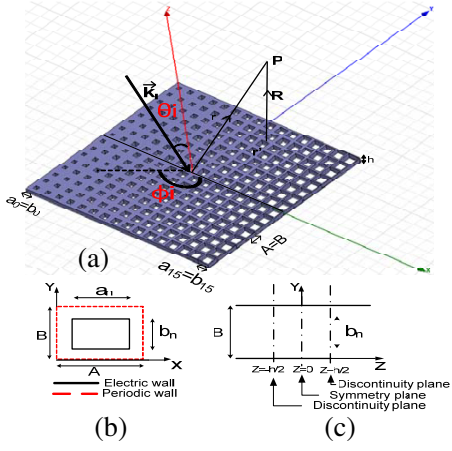

Figure 8. (a) Finite frequency selective surface illuminated by a plane wave under oblique incidence, (b) cross section of the elementary cell, (c) side-view of the cell (all the cells present the same thickness h).

$\vec{J}_{eq}$ defined by the lower-order modes (active modes) [16]. The planar FSS domain is characterized by a surface impedance matrix $[Z_s]$ (which fixes the boundary conditions of the problem).

To determine the solution of the boundary value problem in free space, we are led to calculate the electric field radiated by the equivalent current $\vec{J}_{eq}$. The equivalent current $\vec{J}_{eq}$, using Galerkin procedure, can be expressed on a modal basis:

$$\vec{J}_{eq} = \sum\nolimits_{i=1}^{N*N} \vec{I}_{eq\_i} * \vec{g}_{eq\_i} \tag{6}$$

where $\vec{g}_{eq\_i}$ are the entire domain trial functions and N is the number of trial functions. In the same way the modal expansion $[V^{inc}]$ of the incident filed $\vec{E}^{inc}$ on the planar domain using entire domain trial functions is given by:

$$\left[V^{inc}\right] = \int_{-\infty}^{+\infty} \int_{-\infty}^{+\infty} \vec{g}_{eq\_j}(x,y) * \vec{E}^{inc}(x,y)dxdy \tag{7}$$

Hence, finally the boundary value Equation (4) is given by:

$$\left[V^{inc}\right] - ([Z] * [I_{eq}]) = [Z_s] * [I_{eq}] \tag{8}$$

$[I_{eq}]$ can be written as:

$$[I_{eq}] \left([Z] + [Z_s]\right)^{-1} \left[V^{inc}\right] \tag{9}$$

where $[Z]$ is the modal expansion of the dyadic Green function [23]. This Green function is given by:

$$G(x,y;x',y') = \frac{e^{-jk[(x-x')^2+(y-y')^2]^{1/2}}}{4\pi[(x-x')^2+(y-y')^2]^{1/2}} \tag{10}$$

$[Z]$ can then be found from the following expression obtained by applying Galerkin method.

$$\begin{aligned}[Z]_{i,j} \;=\; & \int_{-\infty}^{+\infty} \int_{-\infty}^{+\infty} \vec{g}_{eq\_i}(x,y)^* \cdot \frac{j}{\omega\varepsilon_0} \begin{bmatrix} k + \frac{\partial^2}{\partial x^2} & \frac{\partial^2}{\partial x \partial y} \\ \frac{\partial^2}{\partial y \partial x} & k + \frac{\partial^2}{\partial y^2} \end{bmatrix} \\ & G(x,y;x',y') * \vec{g}_{eq\_j}\left(x',y'\right) dxdy \end{aligned} \tag{11}$$

The convolution product is given by the following equation:

$$\begin{aligned} & G(x,y;x',y') * g_{eq\_j}(x',y') \\ = & \int_{-\infty}^{+\infty} \int_{-\infty}^{+\infty} \frac{e^{-jk[(x-x')^2+(y-y')^2]^{1/2}}}{4\pi[(x-x')^2+(y-y')^2]^{1/2}} * \vec{g}_{eq\_j}\left(x',y'\right) dx'dy' \end{aligned} \tag{12}$$

It is easier to solve the expression of Equation (11) in the spectral domain rather than in the spatial domain. The double convolution

integral of Equation (12) converts into a simple product in the spectral domain. The goal is to calculate the current $[I_{eq}]$ using Equation (9) which will give the field reflected by the grid. This current can be found if $[Z]$ and $[Z_s]$ are known. The calculation of $[Z]$ is done separately. Once $[Z]$ is calculated and saved, it can be reused for the calculation of the radiation patterns of uniform or non-uniform grids as opposed to the standard electromagnetic solvers which require the calculation to be completely redone whenever there is even a little change in the structure. For the calculation of $[Z_s]$ equal to $[Z_{even}]$ a number of active modes ($N_1 = N_2 = 80$) at all scale levels has been chosen for insuring the numerical convergence of the S-parameters. Figure 9 displays the radiation pattern of the finite-size and thick FSS pictured in Figure 8(a) with a thickness $h = 5\,\text{mm}$ in the case of oblique incidence ($\theta = 20°$, $\varphi = 0°$). Ansoft HFSS [24] (version 12.0.0) based on Finite Element Method was used for comparison purposes with 0.02 as stopping criterion for the adaptive convergence solution. An excellent agreement between the HFSS and SCT results can be observed on a large dynamic range down to $-40\,\text{dB}$ below maximum power with acceptable accuracy.

Following in the Table 1, there is comparison between the computation times of SCT and HFSS for the above FSS. The time comparison is given for different number of cells (N) within the FSS. From the time values, it can be concluded that the simulation time for SCT increases very slowly with respect to the increment in the number of cells as compared to HFSS.

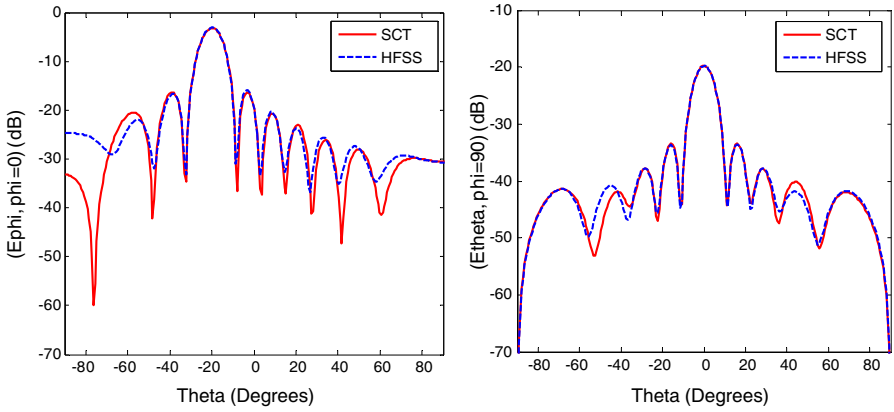

Figure 9. Radiation Pattern (a) E-plane, and (b) H-plane at 10 GHz.

Table 1. Computation time of four different FSSs (thick metallic grids) analyzed by the Scale Changing Technique (SCT) and the Finite Element Method (HFSS).

Number of cells	Computing time non-uniform array(s); $\theta = 20°$, $\varphi = 0°$	
N	SCT	HFSS
4	12	44
16	15	64
64	23	130
256	52	563

3. CONCLUSION

The Scale-Changing Technique has been successfully applied to the global electromagnetic analysis of a finite-size and thick metallic FSS. Very good agreement has been observed between computational results from SCT and FEM implemented in Ansoft HFSS in a very wide frequency band under an oblique incidence plane wave excitation. However the computation time is significantly reduced when using SCT-based software compared with the FEM simulation tool. This paves the way to the implementation of an optimization process, benefiting from large number of parameters available with non-uniform grid to improve overall performances. This gives SCT an advantage over conventional full-wave analysis tools that use linear meshing, especially when simulating large structures where greater number of scales can be defined, e.g., in case of large planar arrays containing hundreds of elements. The modular nature of the approach is exploited by running huge simulations in parallel using distributed computing.

ACKNOWLEDGMENT

This work was supported by French Spatial Agency CNES and Thales Alenia Space Toulouse, France.

REFERENCES

1. Huang, J. and J. A. Encinar, *Reflectarray Antennas*, IEEE Press, 2007.
2. Pozar, D. M. and D. H. Schaubert, "Analysis of an infinite array of rectangular microstrip patches with idealized probe feeds," *IEEE*

Transactions on Antennas and Propagation, Vol. 32, 1101–1107, Oct. 1984.

3. Pozar, D. M., "Analysis of an infinite phased array of aperture coupled microstrip patches," *IEEE Transactions on Antennas and Propagation*, Vol. 37, 418–425, Apr. 1989.
4. Cadoret, D., A. Laisne, R. Gillard, and H. Legay, "Design and measurement of new reflectarray antenna using microstrip patches loaded with slot," *Electronic Letters*, Vol. 41, No. 11, 623–624, May 2005.
5. Mittra, R., C. H. Chan, and T. Cwik, "Techniques for analyzing frequency selective surfaces a review," *Proceedings of IEEE*, Vol. 76, No. 12, 1593–1615, Dec. 1988.
6. Wan, C. and J. A. Encinar, "Efficient computation of generalized scattering matrix for analyzing multilayered periodic structures," *IEEE Transactions on Antennas and Propagation*, Vol. 43, 1233–1242, Oct. 1995.
7. Bardi, I., R. Remski, D. Perry, and Z. Cendes, "Plane wave scattering from frequency selective surfaces by finite element method," *IEEE Transactions Magazine*, Vol. 38, No. 2, 641–644, Mar. 2002.
8. Harms, P., R. Mittra, and K. Wae, "Implementation of periodic boundary condition infinite-difference time-domain algorithm for FSS structures," *IEEE Transactions on Antennas and Propagation*, Vol. 42, 1317–1324, Sep. 1994.
9. Pilz, D. and W. Menzel, "Full wave analysis of a planar reflector antenna," *Asia Pacific Microwave Conference*, Dec. 1997.
10. Sarkar, T. K. and S. M. Rao, "The application of conjugate gradient method for the solution of electromagnetic scattering from arbitrarily oriented wire antennas," *IEEE Transactions on Antennas and Propagation*, Vol. 32, No. 4, 398–403, Apr. 1984.
11. Sarkar, T. K. and S. M. Rao, "An iterative method for solving electrostatic problems," *IEEE Transactions on Antennas and Propagation*, Vol. 30, No. 4, 611–616, Jul. 1982.
12. Mittra, R., J.-F. Ma, E. Lucente, and A. Monorhio, "CBMOM — An iteration free MoM approach for solving large multiscale EM radiation and scattering problems," *IEEE Antennas and Propagation Society International Symposium*, Vol. 2B, 2–5, Jul. 3–8, 2005.
13. Lucente, E., A. Monorchio, and R. Mittra, "Generation of characteristic basis functions by using sparse MoM impedance matrix to construct the solution of large scattering and radiation

problems," *IEEE Antennas and Propagation Society International Symposium*, 4091–4094, 2006.

14. Aubert, H., "The concept of scale-changing network in the global electromagnetic simulation of complex structures," *Progress In Electromagnetics Research B*, Vol. 16, 127–154, 2009.
15. Tao, J. W. and H. Baudrand, "Multimodal variational analysis of uniaxial waveguide discontinuities," *IEEE Transactions on Microwave Theory and Techniques*, Vol. 39, No. 3, 506–516, Mar. 1991.
16. Voyer, D., H. Aubert, and J. David, "Scale-changing technique for the electromagnetic modeling of planar self-similar structures," *IEEE Transactions on Antennas and Propagation*, Vol. 54, 2783–2789, No. 10, Oct. 2006.
17. Voyer, D., H. Aubert, and J. David, "Radar cross section of discrete self-similar objects using a recursive electromagnetic analysis," *IEEE AP-S International Symposium and USNC/URSI National Radio Science Meeting, Monterey*, Vol. 4, 4260–4263, California, USA, Jun. 20–26, 2004.
18. Voyer, D., H. Aubert, and J. David, "Radar cross section of self-similar targets," *Electronics Letters*, Vol. 41, No. 4, 215–217, Feb. 17, 2005.
19. Tahir, F. A., et al., "Full wave analysis of planar structures using scale changing technique under feed horn excitation," *Antennas and Propagation Conference (LAPC)*, 445–448, Loughborough, UK, Nov. 8–9, 2010.
20. Perret, E. and H. Aubert, "A multi-scale technique for the electromagnetic modeling of active antennas," *IEEE AP-S International Symposium on Antennas Propagation and USNC/URSI National Radio Science Meeting*, Vol. 4, 3923–3926, Monterey, California, USA, Jun. 20–25, 2004.
21. Perret, E. and H. Aubert, "Scale-changing technique for the computation of the input impedance of active patch antennas," *IEEE Antennas and Wireless Propagation Letters*, Vol. 4, 326–328, 2005.
22. Collin, R. E., *Field Theory of Guided Waves*, 2nd Edition, 588–591, IEEE Press, 1990.
23. Vardaxoglou, J. C., *Frequency Selective Surfaces*, John Wiley and Sons, 1997.
24. Ansoft HFSS website, http://www.ansoft.com/products/hf/hfss/.